INTERNATIONAL JOURNAL FOR NUMERICAL METHODS IN FLUIDS
Int. J. Numer. Meth. Fluids **29**: 397–410 (1999)

AN OPERATOR SPLITTING NUMERICAL SCHEME FOR THERMAL/ISOTHERMAL INCOMPRESSIBLE VISCOUS FLOWS

BLANCA BERMÚDEZ[a,b] AND ALFREDO NICOLÁS[b,*]

[a] *Facultad de C. Físico-Matemáticas, BUAP, Pue, Mexico*
[b] *Depto. de Matemáticas, UAM-I, 09340 México D.F., Mexico*

SUMMARY

A numerical scheme for time-dependent incompressible viscous fluid flow, thermally coupled under the Boussinesq approximation is presented. The scheme combines an operator splitting in the time discretization and linear finite elements in the space discretization, and is an extension of one previously applied for isothermal incompressible viscous flow governed by the Navier–Stokes equations. To show the efficiency of the scheme, numerical results are presented for mixed convection, and natural convection at high Rayleigh numbers. Restricting the scheme to the isothermal case, some numerical results at high Reynolds numbers are included, i.e. the scheme is tested for a small viscosity and a large force term, which are not trivial tasks to deal with. Copyright © 1999 John Wiley & Sons, Ltd.

KEY WORDS: operator splitting; high Reynolds numbers; high Rayleigh numbers; mixed convection; natural convection

1. INTRODUCTION

For time-dependent thermal and isothermal incompressible viscous flow, governed respectively by the Boussinesq approximation and the Navier–Stokes equations, a numerical scheme is presented that combines an operator splitting in the time discretization and linear finite elements in the space discretization. The operator splitting is based on a second-order time discretization and, like other operator splitting methods, leads to decoupling the difficulties associated with the non-linearities and the incompressibility condition; thus reducing the problem into a sequence of simpler subproblems (with respect to the original one) at each time step: Stokes-type and transport-type (advection–diffusion) problems.

The operator splitting used is an extension of one previously applied to isothermal flows only [1–3]. Analogously, as in the isothermal case, in the middle step of the splitting, uncoupled scalar advection–diffusion problems are found; then, advantage is taken of an appropriate classical upwind technique for the velocity in order to handle high Rayleigh and Reynolds numbers. This corresponds to a small viscosity and a large force term in the momentum equations, which, as is well-known, is not a trivial task to deal with. In the case under consideration, the large force term is also coupled with the temperature equation.

* Correspondence to: Depto. de Matemáticas, UAM-I, 09340 México D.F., México.

CCC 0271–2091/99/040397–14$17.50

Received 3 February 1997
Revised 31 March 1998

The main goal of this paper is to show that the scheme proposed is able to reproduce the main characteristics of the flow with coarse meshes; these characteristics agree well with those reported by other schemes [4–10] using finer meshes. It is worth mentioning that the size of the coarse meshes are such that it makes a big difference in CPU time and memory savings, see Section 5.

For the Boussinesq model, numerical results are presented for mixed and natural convection. The results for mixed convection agree well with those reported in [6], where a finite difference package is used. For natural convection, results for Rayleigh numbers in the range $10^3 \leq Ra \leq 10^8$ are presented; they compare well with those in FIDAP and those recently reported in [7] (note that the results reported in FIDAP and [7] correspond to $10^3 \leq Ra \leq 10^6$ only). As mentioned before, linear finite elements are used, whereas in FIDAP and [7] higher-order ones are used.

Restricting the scheme to isothermal flow, results are shown for Reynolds numbers $Re \geq 15000$, which are higher than those in [1–3]. These results can not be compared with other published works, since for the few results obtained, there is not enough evidence that they represent the correct flow for this range of Reynolds numbers. The validation of the results relies on the fact that for smaller Reynolds numbers, and up to some coarse meshes, the same correct and accurate results have been obtained as other authors got with finer meshes [1–3]. Moreover, whenever the Reynolds number increases, the scheme does not require any special treatment other than to decrease the time step, which is a natural requirement of the fast dynamics of the flow. Taking into consideration that, for $Re \geq 5000$, the results may depend on the method [8,9], and that for high Re, the steady state may not exist [11], and even a steady laminar solution may not exist for $Re = Rc$, with $5000 \leq Rc \leq 10000$ as conjectured in [8], it could be said that these are the results the numerical scheme provides for the initial condition chosen.

For a small viscosity or a large force term, the numerical scheme is able to achieve the results directly, either starting from $t = 0$ or from previously computed results for smaller values of the parameter (Reynolds or Rayleigh number). Usually, other schemes have to start from a previous computed value.

Until now, the numerical scheme has not been tested with really non-steady benchmarks problems. However, with a previous isothermal version of this scheme, where the advection step is treated as non-linear and no upwinding effect is used, a double jet time-dependent problem works quite well with a fine mesh [12]. The next step should be to apply the scheme to this isothermal problem, as well as to some thermal time-dependent ones, like buoyant plumes problems [13]. Moreover, based on the fact that the scheme can start from $t = 0$ regardless of the size of the viscosity, and, as mentioned above, that for high Reynolds numbers the steady state may not exist, the result presented for $Re = 40000$ (Section 5), may be considered as a time-dependent one.

2. THE CONTINUOUS PROBLEM

Let $\Omega \subset R^N$ $(N = 2, 3)$ be the region of the flow, and Γ its boundary. The time-dependent, dimensionless equations for a thermal fluid flow based on the Boussinesq approximation are given by

$$\frac{\partial \mathbf{u}}{\partial t} - \frac{1}{Re}\,\Delta \mathbf{u} + (\mathbf{u} \cdot \nabla)\mathbf{u} + \nabla p = \frac{Ra}{Pr\,Re^2}\,T\boldsymbol{g}, \quad \mathbf{x} \in \Omega, \quad t > 0; \tag{2.1}$$

$$\nabla \cdot \mathbf{u} = 0, \quad \mathbf{x} \in \Omega, \quad t > 0 \quad \text{(incompressibility condition)}; \tag{2.2}$$

$$\frac{\partial T}{\partial t} - \frac{1}{Re\ Pr}\Delta T + (\mathbf{u}\cdot\nabla)T = 0, \quad \mathbf{x}\in\Omega, \quad t>0; \tag{2.3}$$

where $\mathbf{u}$, p and T are the velocity, pressure and temperature of the flow respectively. Ra is the Rayleigh number, Pr is the Prandtl number, and $\boldsymbol{g}$ is the gravity vector $\boldsymbol{g}=(0,1)$. Re is the Reynolds number; as is known, $1/Re=\nu$, where ν is the viscosity.

The momentum equation (2.1) and the temperature equation (2.3) should be supplemented with appropriate initial and boundary conditions, say for instance

$$\mathbf{u}(\mathbf{x},0)=\mathbf{u}_0(\mathbf{x}) \quad \text{a.e. in } \Omega \ (\nabla\cdot\mathbf{u}_0=0), \tag{2.4}$$

$$T(\mathbf{x},0)=T_0(\mathbf{x}) \quad \text{a.e. in } \Omega, \tag{2.5}$$

$$\mathbf{u}=\mathbf{f}_1 \text{ on } \Gamma, \quad t\geq 0 \quad \left(\int_\Gamma \mathbf{f}_1\cdot\mathbf{n}\,\mathrm{d}T=0\right), \tag{2.6}$$

$$T=f_2 \text{ on } \Gamma, \quad t\geq 0. \tag{2.7}$$

Remarks:

(1) The coupling between (2.1) and (2.3) involving Re corresponds to *mixed convection*. For *natural convection*, $Re=1$ is taken.

(2) For the Navier–Stokes equations, there is no coupling with the energy equation, and the right-hand-side of (2.1) is T-independent, and therefore, independent of the parameters Ra, Pr and Re.

For thermally coupled flows, to the difficulties of the Navier–Stokes problem, see [1–3], the coupling between Equations (2.1)–(2.3) are added. Through an operator splitting process, the difficulties associated with the non-linearities and the incompressibility condition are decoupled.

3. TIME DISCRETIZATION AND AN OPERATOR SPLITTING PROCESS

For the time discretization, the time derivatives $\mathbf{u}_t$ and T_t are approximated by the second-order scheme

$$f_t(\mathbf{x},(n+1)\Delta t)\approx\frac{1.5f^{n+1}-2f^n+0.5f^{n-1}}{\Delta t}, \quad n\geq 1,$$

where f^k is an approximation for an enough smooth function f at $(\mathbf{x},k\Delta t)$.

The time interval is subdivided from $n\,\Delta t$ to $(n+1)\,\Delta t$ in three subintervals of equal length $\Delta t/3$, then Equations (2.1)–(2.7) are split in the following form

$$\begin{cases} \text{find } \mathbf{u}^{n+1/3},\ p^{n+1/3}: \\ \dfrac{1.5\mathbf{u}^{n+1/3}-2\mathbf{u}^n+0.5\mathbf{u}^{n-1/3}}{\Delta t/3}-\dfrac{\nu}{2}\Delta\mathbf{u}^{n+1/3}+\nabla p^{n+1/3} \\ =\dfrac{Ra}{Pr\ Re^2}T^n\boldsymbol{g}+\dfrac{\nu}{2}\Delta\mathbf{u}^n-(\mathbf{u}^n\cdot\nabla)\mathbf{u}^n \text{ in } \Omega, \\ \nabla\cdot\mathbf{u}^{n+1/3}=0 \text{ in } \Omega, \\ \mathbf{u}^{n+1/3}=\mathbf{f}_1^{n+1/3} \text{ on } \Gamma, \end{cases} \tag{3.1.1}$$

$$\begin{cases} \text{find } T^{n+1/3}: \\ \dfrac{1.5T^{n+1/3}-2T^{n}+0.5T^{n-1/3}}{\Delta t/3}-\dfrac{\mu}{2}\Delta T^{n+1/3}+(\mathbf{u}^{n+1/3}\cdot\nabla)T^{n+1/3} \\ =\dfrac{\mu}{2}\Delta T^{n} \text{ in } \Omega, \\ T^{n+1/3}=f_2^{n+1/3} \text{ on } \Gamma. \end{cases} \tag{3.1.2}$$

$$\begin{cases} \text{find } u^{n+2/3} \text{ and } T^{n+2/3}: \\ \dfrac{1.5\mathbf{u}^{n+2/3}-2\mathbf{u}^{n+1/3}+0.5\mathbf{u}^{n}}{\Delta t/3}-\dfrac{v}{2}\Delta\mathbf{u}^{n+2/3}+(\mathbf{u}^{n+1/3}\cdot\nabla)\mathbf{u}^{n+2/3} \\ -\dfrac{Ra}{Pr\,Re^2}T^{n+2/3}\boldsymbol{g}=\dfrac{v}{2}\Delta\mathbf{u}^{n+1/3}-\nabla p^{n+1/3} \text{ in } \Omega, \\ \mathbf{u}^{n+2/3}=\mathbf{f}_1^{n+2/3} \text{ on } \Gamma, \\ \dfrac{1.5T^{n+2/3}-2T^{n+1/3}+0.5T^{n}}{\Delta t/3}-\dfrac{\mu}{3}\Delta T^{n+2/3}+(\mathbf{u}^{n+2/3}\cdot\nabla)T^{n+2/3} \\ =\dfrac{\mu}{3}\Delta T^{n+1/3} \text{ in } \Omega, \\ T^{n+2/3}=f_2^{n+2/3} \text{ on } \Gamma. \end{cases} \tag{3.1.3}$$

$$\begin{cases} \text{find } \mathbf{u}^{n+1},\ p^{n+1}: \\ \dfrac{1.5\mathbf{u}^{n+1}-2\mathbf{u}^{n+2/3}+0.5\mathbf{u}^{n+1/3}}{\Delta t/3}-\dfrac{v}{2}\Delta\mathbf{u}^{n+1}+\nabla p^{n+1} \\ =\dfrac{Ra}{Pr\,Re^2}T^{n+2/3}\boldsymbol{g}+\dfrac{v}{2}\Delta\mathbf{u}^{n+2/3}-(\mathbf{u}^{n+2/3}\cdot\nabla)\mathbf{u}^{n+2/3} \text{ in } \Omega, \\ \nabla\cdot\mathbf{u}^{n+1}=0 \text{ in } \Omega, \\ \mathbf{u}^{n+1}=\mathbf{f}_1^{n+1} \text{ on } \Gamma. \end{cases} \tag{3.1.4}$$

$$\begin{cases} \text{find } T^{n+1}: \\ \dfrac{1.5T^{n+1}-2T^{n+2/3}+0.5T^{n+1/3}}{\Delta t/3}-\dfrac{\mu}{2}\Delta T^{n+1}+(\mathbf{u}^{n+1}\cdot\nabla)T^{n+1} \\ =\dfrac{\mu}{2}\Delta T^{n+2/3} \text{ in } \Omega, \\ T^{n+1}=f_2^{n+1} \text{ on } \Gamma, \end{cases} \tag{3.1.5}$$

where $\mu = 1/Pr\,Re$.

Then, denoting the corresponding right-hand-sides by $\mathbf{f}$ and f, it is observed that at each time step, subproblems of the following type have to be solved:
In the first and third subintervals, two Stokes problems

$$\alpha\mathbf{u}-\beta\Delta\mathbf{u}+\nabla p=\mathbf{f} \text{ in } \Omega, \qquad \nabla\cdot\mathbf{u}=0 \text{ in } \Omega, \quad \mathbf{u}=\mathbf{f}_1 \text{ on } \Gamma, \tag{3.2}$$

and two linear advection–diffusion problems for the temperature T

$$\alpha T - \gamma \Delta T + (\mathbf{u} \cdot \nabla) T = f \text{ in } \Omega, \quad T = f_2 \text{ on } \Gamma, \tag{3.3}$$

where $\alpha = 4.5/\Delta t$, $\beta = \nu/2$ and $\gamma = \mu/2$ in Equation (3.3), $\mathbf{u}$ is the velocity from Equation (3.2). In the middle subinterval, a non-linear advection–diffusion system

$$\begin{cases} \alpha T - \gamma \Delta T + (\mathbf{u} \cdot \nabla) T = f \text{ in } \Omega, \quad T = f_2 \text{ on } \Gamma, \\ \alpha \mathbf{u} - \beta \Delta \mathbf{u} + (\mathbf{w} \cdot \nabla) \mathbf{u} - CT\boldsymbol{g} = \mathbf{f} \text{ in } \Omega, \quad \mathbf{u} = \mathbf{f}_1 \text{ on } \Gamma, \end{cases} \tag{3.4}$$

where $\mathbf{w} = \mathbf{u}^{n+1/3}$ and $C = Ra/Pr\, Re^2$.

Remarks:

(1) For natural convection problems, the scheme also works if $(\mathbf{w} \cdot \nabla) T$ is considered instead of $(\mathbf{u} \cdot \nabla) T$ in (3.4), and if T is considered as the temperature previously computed in the momentum equation. However, for mixed convection this uncoupled way between energy and momentum does not work.

(2) For the Navier–Stokes problem, the temperature equations in (3.1.1)–(3.1.5) must be eliminated, and the term $-CT\boldsymbol{g}$ does not appear in (3.4).

4. SOLUTION OF THE STEADY SUBPROBLEMS AND SPACE DISCRETIZATION

As in the isothermal case [1–3], to solve problems of the form (3.2), the efficient technique of the functional equation satisfied by the pressure is used, which is also used in the Glowinski θ-scheme for the corresponding Stokes problem [14,15]; i.e. conjugate gradient is applied on the variational formulation of such an equation. This technique turns out to be also efficient in the context presented here.

Problems of the form (3.3) are equivalent to

$$R_{\mathbf{w}}(T) = 0 \text{ in } \Omega, \quad T = f_2 \text{ on } \Gamma, \tag{4.1}$$

where

$$R_{\mathbf{w}}(T) \equiv (\alpha \mathrm{I} - \gamma \Delta) T + (\mathbf{w} \cdot \nabla) T - f.$$

Equation (4.1) is solved by the fixed point iterative technique given by:

with $T^0 = T_0$ given, solve until convergence

$$T^{m+1} = T^m - \rho (\alpha \mathrm{I} - \gamma \Delta)^{-1} R_{\mathbf{w}}(T^m) \text{ in } \Omega; \quad \rho > 0, \quad T^{m+1} = f_2 \text{ on } \Gamma, \tag{4.2}$$

and then take $T^{n+1/3}$ (or T^{n+1}) $= T^{m+1}$.

Now, defining

$$R(T, \mathbf{u}) \equiv (\alpha \mathrm{I} - \gamma \Delta) T + (\mathbf{u} \cdot \nabla) T - f$$

and

$$\mathbf{R}_{\mathbf{w}}(\mathbf{u}, T) = \alpha \mathbf{u} - \mu \Delta \mathbf{u} + (\mathbf{w} \cdot \nabla) \mathbf{u} - CT\boldsymbol{g} - \mathbf{f}.$$

It is observed that systems of the form (3.4) are equivalent to

$$\begin{cases} R(T, \mathbf{u}) = 0 \text{ in } \Omega, \quad T = f_2 \text{ on } \Gamma, \\ \mathbf{R}_{\mathbf{w}}(\mathbf{u}, T) = 0 \text{ in } \Omega, \quad \mathbf{u} = \mathbf{f}_1 \text{ on } \Gamma. \end{cases} \tag{4.3}$$

Equation (4.3) is solved by the following coupled fixed point iterative process:

with $T^0 = T^{n+1/3}$ and $\mathbf{u}^0 = \mathbf{u}^{n+1/3}$, solve until convergence

$$\begin{cases} T^{m+1} = T^m - \rho(\alpha \mathrm{I} - \gamma\Delta)^{-1} R(T^m, \mathbf{u}^m) \text{ in } \Omega, \\ T^{m+1} = f_2 \text{ on } \Gamma, \\ \\ \mathbf{u}^{m+1} = \mathbf{u}^m - \rho(\alpha \mathrm{I} - \beta\Delta)^{-1} \mathbf{R}_{\mathbf{w}}(\mathbf{u}^m, T^{m+1}) \text{ in } \Omega; \quad \rho > 0, \\ \mathbf{u}^{m+1} = \mathbf{f}_1 \text{ on } \Gamma, \end{cases} \tag{4.4}$$

and then take $T^{n+2/3} = T^{m+1}$, $\mathbf{u}^{n+2/3} = \mathbf{u}^{m+1}$.

Considering $\mathbf{R}_{\mathbf{w}}(\mathbf{u}, T)$ in (4.3) component-wise, one can see that problem (4.4) is equivalent to

$$\begin{cases} (\alpha \mathrm{I} - \gamma\Delta) T^{m+1} = (\alpha \mathrm{I} - \gamma\Delta) T^m - \rho R(T^m, \mathbf{u}^m) \text{ in } \Omega, \\ T^{m+1} = f_2 \text{ on } \Gamma, \\ \\ (\alpha \mathrm{I} - \beta\Delta) u_i^{m+1} = (\alpha \mathrm{I} - \beta\Delta) u_i^m - \rho R_{i\mathbf{w}}(\mathbf{u}^m, T^{m+1}) \text{ in } \Omega; \quad \rho > 0, \\ u_i^{m+1} = f_{1i} \text{ on } \Gamma; \quad i = 1, \ldots, N. \end{cases} \tag{4.5}$$

Therefore, at each iteration, $N+1$ linear problems associated with symmetric elliptic operators have to be solved: *one* problem for the operator $\alpha \mathrm{I} - \gamma\Delta$ and N for $\alpha \mathrm{I} - \beta\Delta$. At each time step, *two* more problems must be counted (one for each (3.1.2) and (3.1.5)) at each iteration of (4.2) associated with the operator $\alpha \mathrm{I} - \gamma\Delta$.

Remarks:

(1) For the uncoupled way in natural convection mentioned in Remark (1) (Section 3), the iterative process (4.4) works uncoupled.

(2) For the Navier–Stokes problems, the temperature relation in the previous fixed point algorithm has to be eliminated.

(3) Unlike the Navier–Stokes problems, the N uncoupled scalar linear advection–diffusion problems for velocity (with temperature influence) in (3.4) are coupled with the non-linear temperature equation through $\mathbf{u}$ and T. However, upwinding in such a situation still works fine, maybe because at each iteration of (4.4) they are uncoupled.

(4) Mentioned in [1–3], the results for the Navier–Stokes equations with coarse meshes reported therein depend strongly on combining upwind and cubic interpolation to initialize (4.4); i.e. if, in the advection–diffusion step, some appropriate upstream information of the flow as well as some memory (to compensate its infinitely short memory [16]) are taken into account. Note that the results reported here for $Re \geq 15000$ depend also on such a combination as far as the corresponding coarse meshes is concerned.

(5) A fixed point iterative process has been used to solve the advection–diffusion problems, to avoid the non-symmetric part of the elliptic operator and because it is cheaper than the conjugate gradient method used by the least-square technique in the corresponding advective subproblems appearing in Glowinski's θ-scheme, see [3] for instance. In this way, elliptic solvers are relied upon, even for the Stokes subproblems. Presently, there is no claim that this is more efficient than other schemes applying sophisticated non-symmetric preconditioners.

For the linear part of the velocity (of advection–diffusion type) in (3.4), the second-order-accurate Ikeda partial upwind [17] is used, which introduces the minimum amount of artificial

viscosity needed to preserve the discrete maximum principle, the discrete mass conservation law, and the $L_\infty(\overline{\Omega})$ convergence.

The space discretization is based on finite elements; therefore, variational formulations have to be given for the steady subproblems and then restrict these formulations to appropriate finite element spaces. Like in [1–3], linear finite elements are used. For velocity and temperature, a mesh twice finer than the one for the pressure is used.

5. NUMERICAL RESULTS

The step mesh size for velocity and temperature is denoted h_v, and the results shown correspond to steady state flow (from the non-steady problem).

The results of this paper are compared with those in [4–10]. A description follows.

First, a mixed convection problem in a driven cavity is solved, with a stable vertical temperature gradient as reported in [6], where numerical results are presented over broad ranges of the parameters, $0 \leq Ra \leq 10^6$ and $400 \leq Re \leq 3000$, using the MAC finite difference package. They identify in this way the major dynamic elements in various regimes of the parameters. Two cases are studied in terms of the Grashof number Gr: the case when $Gr/Re^2 \leq 1$, where the features of the flow are similar to the ones of a conventional driven-cavity of a non-stratified fluid; fluids are well-mixed and temperature variations are small. In the other case, when $Gr/Re^2 \geq 1$, much of the middle and bottom portions of the cavity interior are stagnant.

Note here that the dimensionless Grashof number Gr is given by $Gr = Ra/Pr$; then, when replacing it in the momentum equation (2.1), the right-hand-side turns out to be $(Gr/Re^2)\boldsymbol{Tg}$.

For the first case, the isotherms and streamlines are shown in Figure 1 for $Gr = 100$ and $Re = 1000$, with $h_v = \frac{1}{32}$. In Figure 2, for the same value of Gr but $Re = 4000$, with $h_v = \frac{1}{48}$. In [6], $h_v = \frac{1}{128}$ and $\frac{1}{256}$ are used. For the second case, in Figure 3, the isotherms and streamlines are shown for $Re = 1000$ and $Gr = 10^6$ with $h_v = \frac{1}{32}$. In [6], $h_v = \frac{1}{64}$, $\frac{1}{128}$ and $\frac{1}{256}$ are used.

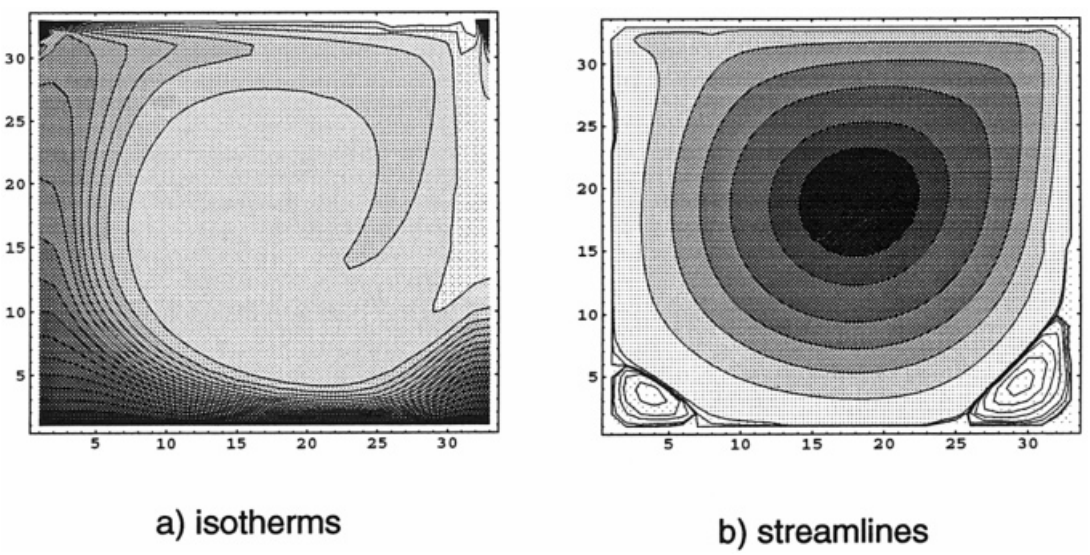

Figure 1. The isotherms and streamlines for $Gr = 100$ and $Re = 1000$, with $h_v = \frac{1}{32}$.

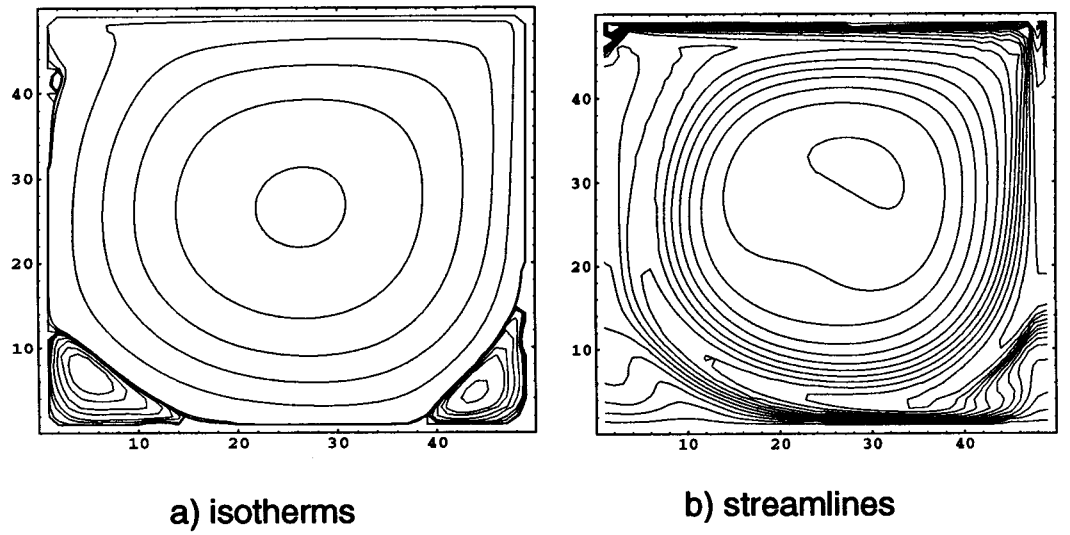

Figure 2. The isotherms and streamlines for $Gr = 100$ and $Re = 4000$, with $h_v = \frac{1}{48}$.

The results agree well with those in [6], even with the significant difference in mesh size; moreover, concerning the first case, like in [1–3], there is no evidence that the scheme here cannot accurately reproduce results for $Re > 4000$.

Next, for natural convection, the problem of the buoyancy-driven flow in a square cavity with vertical side walls differentially heated is solved. This problem is solved by FIDAP (a well-known finite element package), which has a steady state Boussinesq solver and uses a fully coupled method. As mentioned in Section 1, the Rayleigh number range is $10^3 \leq Ra \leq 10^6$. To obtain the solution for $Ra = 1000000$, FIDAP has to perform a sequence of solutions for $Ra = 1000$, 10000, 100000, and take the solution from the previous Ra number as the starting

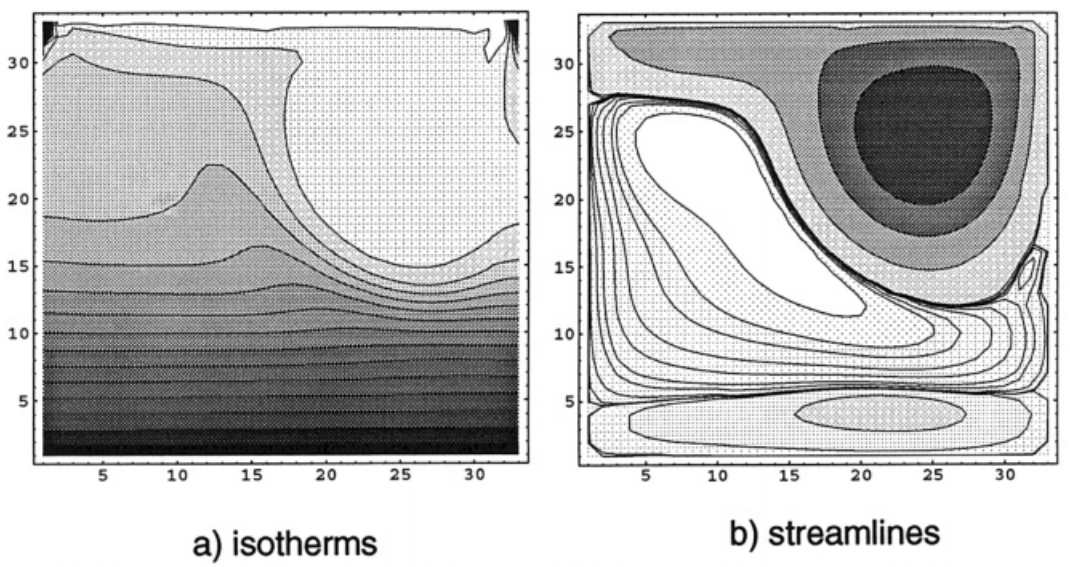

Figure 3. The isotherms and streamlines for $Gr = 10^6$ and $Re = 1000$, with $h_v = \frac{1}{32}$.

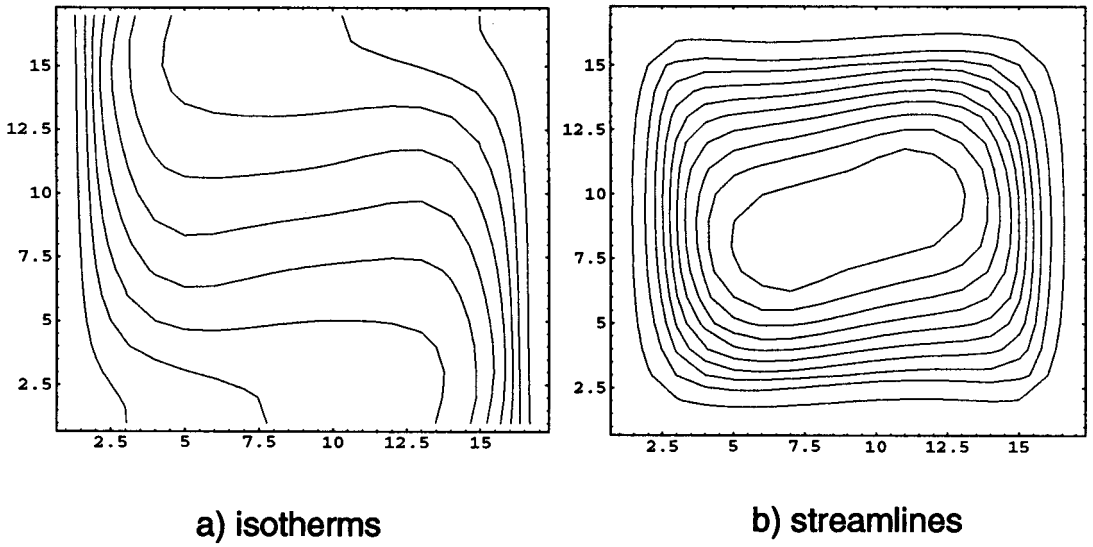

Figure 4. The isotherms and streamlines for $Ra = 10^5$, with $h_v = \frac{1}{16}$.

value for higher *Ra*. The mesh used is irregular and finer than the one used in this work. FIDAP uses 576 rectangular elements with 1825 nodes, and a very coarse regular mesh is used, $h_v = \frac{1}{16}$ here, which corresponds to 289 nodes.

In Figures 4–7, the isotherms and the streamlines are shown for $Ra = 10^5$, 10^6, 10^7 and 10^8; all of them with $h_v = \frac{1}{16}$.

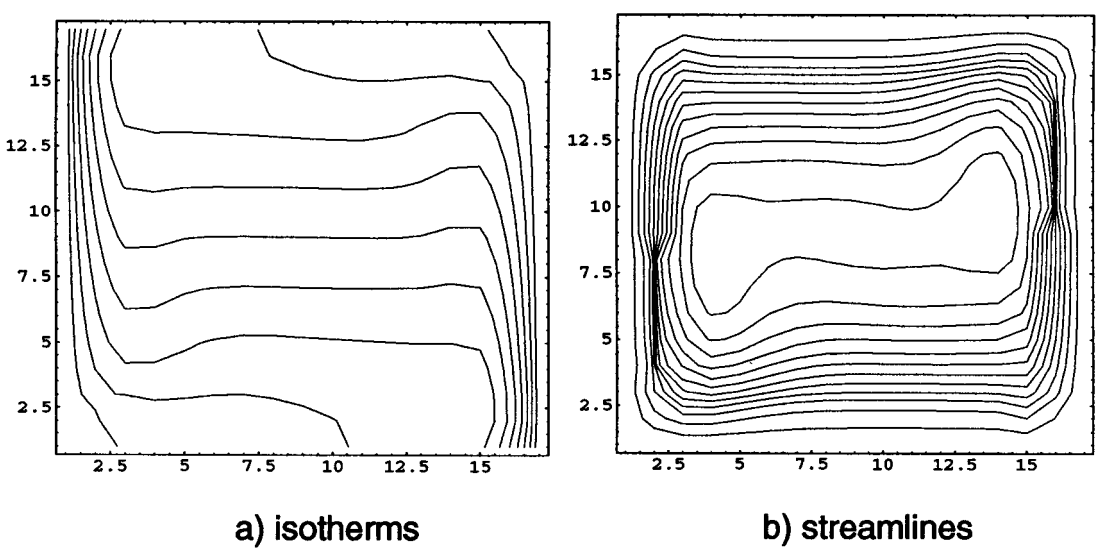

Figure 5. The isotherms and streamlines for $Ra = 10^6$, with $h_v = \frac{1}{16}$.

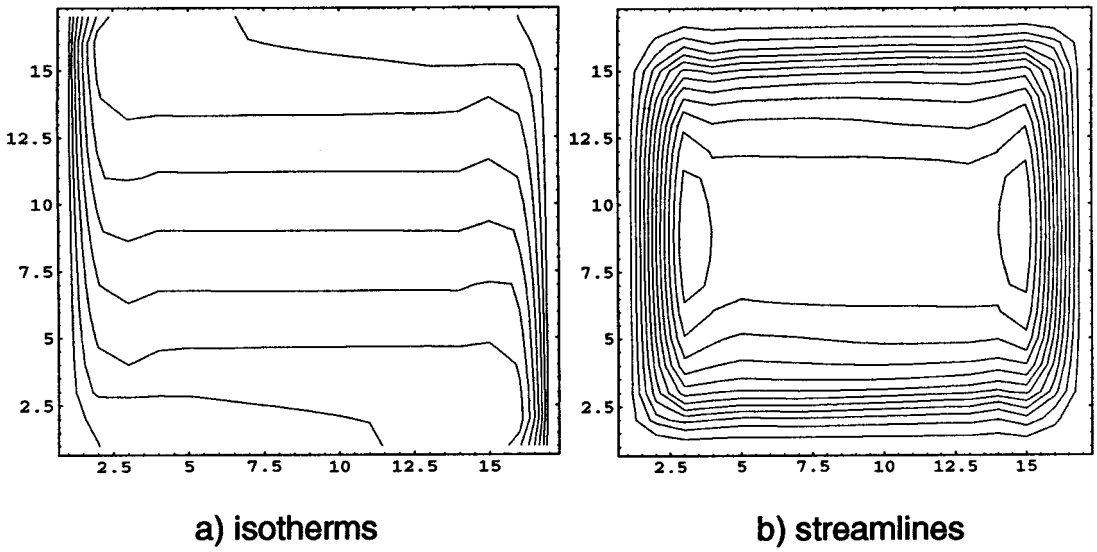

Figure 6. The isotherms and streamlines for $Ra = 10^7$, with $h_v = \frac{1}{16}$.

Remark:

(1) All these results were also obtained with $h_v = \frac{1}{32}$ and they look identical.

FIDAP compares its results with results in [4]; [5] and [7] with FIDAP; and [5] with [10]. All these works but [4] use the primitive variables formulation (velocity and pressure). The reference work [4] uses the Boussinesq steady state vorticity–streamfunction formulation.

In [5], the problem is solved investigating different numerical schemes, constructed on the iterative explicit and semi-implicit bases, and using the concept of Lagrange multiplier. The cavity here is covered by a rectangular mesh of graded elements. They use 25×25 biquadratic/

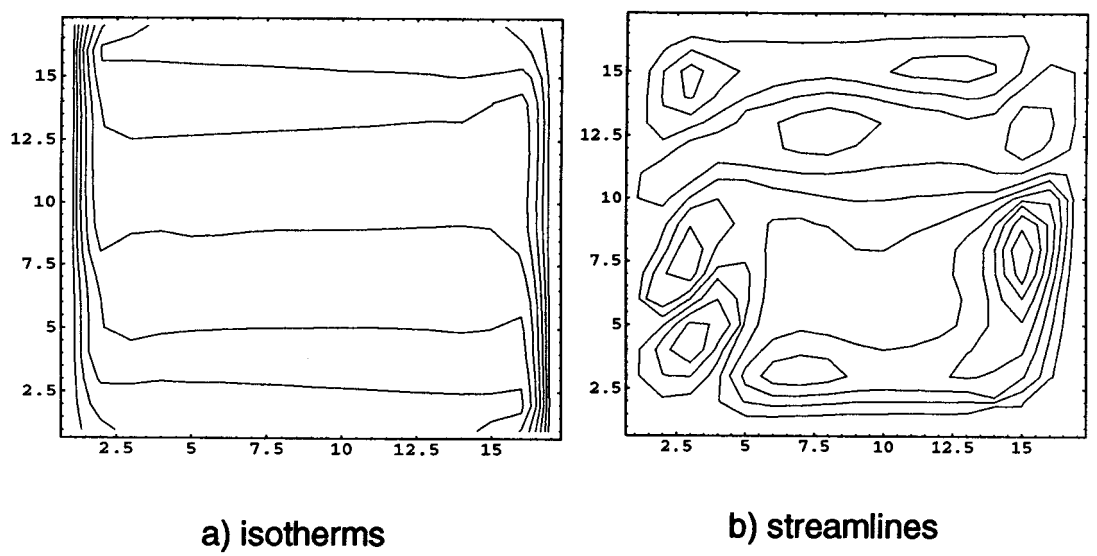

Figure 7. The isotherms and streamlines for $Ra = 10^8$, with $h_v = \frac{1}{16}$.

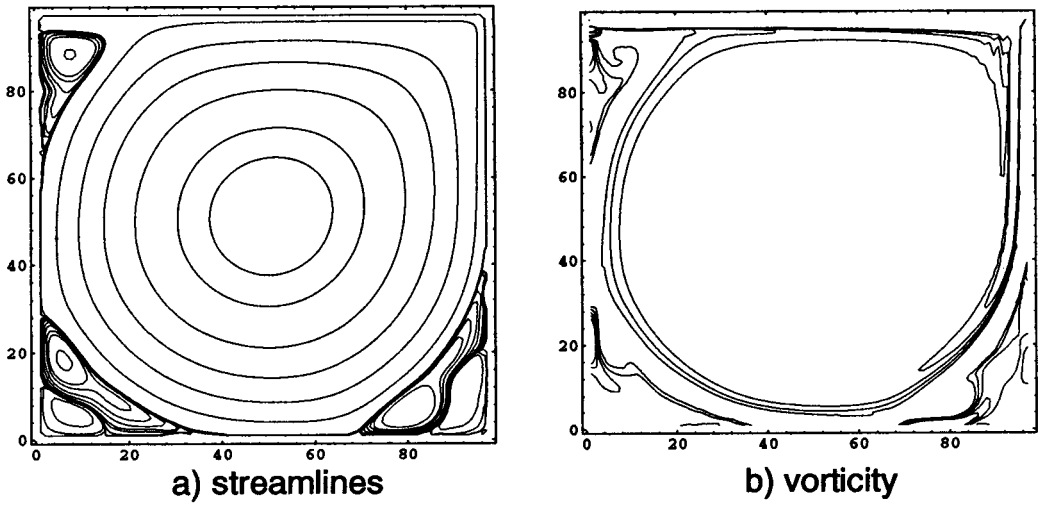

Figure 8. The streamlines and vorticity for $Re = 15000$, with $h_v = \frac{1}{96}$.

bilinear elements for velocity and pressure. In [10], results are shown with a least-squares finite element method with 50×50 bilinear elements. In [7], an operator splitting method designed for compressible flow at low Mach number is used; the mesh reported is the same as the one used by FIDAP.

For the Navier–Stokes equations, the familiar driven cavity flow test problem is considered. In Figure 8, the streamlines and vorticity for are shown for $Re = 15000$ with $h_v = \frac{1}{96}$. In [8], the streamlines are shown for this Reynolds number (from the steady problem) with a $\frac{1}{256} \times \frac{1}{256}$ mesh. There is a perfect agreement with the central vortex despite the big difference in mesh size. In Figures 9 and 10, the streamlines and vorticity are shown for $Re = 20000$ and 40000, both with $h_v = \frac{1}{128}$. The result for $Re = 40000$ is not yet at the steady state, if any. Nevertheless,

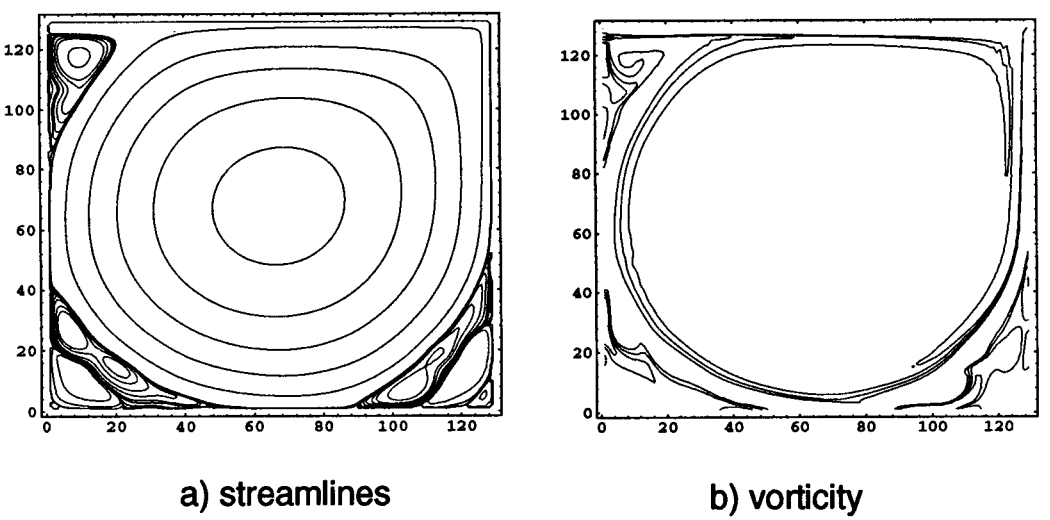

Figure 9. The streamlines and vorticity for $Re = 20000$, with $h_v = \frac{1}{128}$.

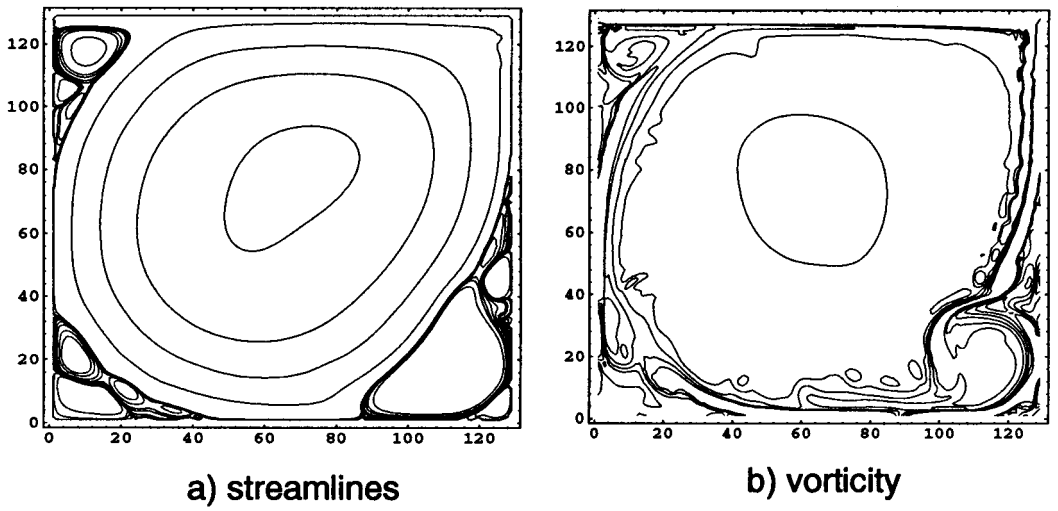

Figure 10. The streamlines and vorticity for $Re = 40000$, with $h_v = \frac{1}{128}$.

it shows an expected structure for the flow; it is presented like this because it was started from $t = 0$. As discussed in [8], the knowledge of flows at high Reynolds numbers may give some answers on turbulent flows.

Just to give an idea about CPU times, Table I shows some of them for the natural convection problem, where the computations (like all the other ones reported here) were made on the Power Challenger supercomputer at UAM-I (México). The code only takes the default optimization of the machine, i.e. it is not a parallel code.

Remark:

(2) With $h_v = \frac{1}{16}$, the program can also run in a Pentium PC, at 166 MHz, for the natural convection problem; for instance, for $Ra = 1000$, it takes almost 24 h.

6. CONCLUSIONS

This paper presents an operator numerical scheme for thermal/isothermal time-dependent incompressible viscous flows. Based on its methodology and computational performance, some conclusions are:

Table I. CPU time for the natural convection problem

Rayleigh	h_v	Time (h)
1000	$\frac{1}{16}$	4
1000	$\frac{1}{32}$	10
10 000	$\frac{1}{16}$	6
10 000	$\frac{1}{32}$	12
100 000	$\frac{1}{16}$	10
100 000	$\frac{1}{32}$	15
1 000 000	$\frac{1}{16}$	15
1 000 000	$\frac{1}{32}$	19

(1) It uses the primitive variables formulation, and, once the problem is split in the time discretization, the solution of the steady subproblems is based on iterative techniques, which in turn relies on the solution of linear elliptic problems. Then its application in 3D problems is quite clear; however, some limitations may exist on the computational effort.

(2) It shows good stability for critical values of the parameters (high Rayleigh and Reynolds numbers). This can be seen from the results for $Ra = 10^8$ in natural convection and $Re = 40\,000$ for isothermal flow. It is also noteworthy that such stability holds even if computing is started from $t = 0$, regardless of the values of the parameters.

(3) The results obtained with significantly coarse meshes makes the scheme suitable for more complicated memory demanding flows, as long as they preserve the incompressible structure; for instance, ocean, atmospheric and coupled ocean–atmosphere flows (after Boussinesq approximation and transformation to pressure co-ordinates are applied) [18–20]. As already mentioned in [1–3], such robustness with coarse meshes can also be advantageous for the associated memory demanding control problems [15,21,22].

ACKNOWLEDGMENTS

The authors would like to thank the remarks of the anonymous referees that have improved the presentation of the paper. They also wish to thank Professor R. Glowinski for his comments and encouragement.

REFERENCES

1. B. Bermúdez, A. Nicolás and F.J. Sánchez, 'On operator splitting with upwinding for the unsteady Navier–Stokes equations', *East–West J. Numer. Math.*, **4**, 83–98 (1996).
2. A. Nicolás, F.J. Sánchez and B. Bermúdez, 'On operator splitting for the Navier–Stokes equations at high Reynolds numbers', in J.A. Désidéri, C. Hirsch, P. Le Tallec, M. Pandolfi and J. Periaux (eds.), *Third ECCOMAS Computational Fluid Dynamics Conference 96*, Wiley, New York, 1996, pp. 85–89.
3. B. Bermúdez, A. Nicolás, F.J. Sánchez and E. Buendía, 'Operator splitting and upwinding for the Navier–Stokes equations', *Computational Mechanics 20*, Springer, Berlin, 1997, pp. 474–477.
4. G. de Vahl Davis, 'Natural convection in a square cavity—a benchmark solution', *Int. J. Numer. Methods Fluids*, **3**, 249–264 (1983).
5. B. Ramaswamy, T.C. Jue and J.E. Akin, 'Semi-implicit and explicit finite element schemes for coupled fluid/thermal problems', *Int. J. Numer. Methods Eng.*, **34**, 675–696 (1992).
6. R. Iwatsu, Jae Min Hyn and Kunio Kuwahara, 'Mixed convection in a driven cavity with a stable vertical temperature gradient', *Int. J. Heat Transf.*, **36**, 1601–1608 (1993).
7. Chin-Hsien Li and Roland Glowinski, 'Modeling and numerical simulation of low Mach number compressible flows', *Int. J. Numer. Methods Fluids*, **23**, 77–103 (1996).
8. C.-H. Bruneau and C. Jouron, 'An efficient scheme for solving steady incompressible Navier–Stokes equations', *J. Comp. Phys.*, **89**, 389–413 (1990).
9. H. Huang and B.R. Seymour, 'The no-slip boundary condition in finite difference approximations', *Int. J. Numer. Methods Fluids*, **22**, 713–729 (1996).
10. L.Q. Tang and T.H. Tsang, 'A least-squares finite element method for time-dependent incompressible flows with thermal convection', *Int. J. Numer. Methods Fluids*, **17**, 271–289 (1993).
11. B. Mohammadi and O. Pironneau, *Analysis of the K–Epsilon Turbulence Model*, Wiley, New York, 1994.
12. A. Nicolas-Carrizosa and F. Sanchez-Bernabe, 'Ecuaciones de Navier–Stokes no Estacionarias: Un Esquema de Descomposicion de Operadores', *Inform. Tecnol.*, **7**, 133–137 (1996).
13. P.D. Minev, F.N. van de Vosse, L.J.P. Timmermans, C.C.M. Rindt and A.A. Steenhoven, 'Numerical simulation of buoyant plumes using a spectral element technique', in L.C. Wrobel, C.A. Brebbia and A.J. Nowak (eds.), *Advanced Computational Methods in Heat Transfer III*, Computational Mechanics Publications, Southampton, 1994, pp. 147–154.
14. R. Glowinski, *Numerical Methods for Non-linear Variational Problems*, Springer, Berlin, 1990.
15. R. Glowinski, 'Finite element methods for the numerical simulation of incompressible viscous flow. Introduction to the control of the Navier–Stokes equations', in: *Lectures in Applied Mathematics*, vol. 28, AMS, Providence, RI, 1991.
16. R. Dautray and J.L. Lions, *Mathematical Analysis and Numerical Methods for Science and Technology*, Springer, New York, 1985.

17. T. Ikeda, *Maximum Principle in Finite Elements Models for Convection–Diffusion Phenomena*, North-Holland, Amsterdam, 1983.
18. J.L. Lions, R. Temam and S. Wang, 'New formulation of the primitive equations of atmosphere and applications', *Non-linearity*, **5**, 237–288 (1992).
19. J.L. Lions, R. Temam and S. Wang, 'On the equations of the large-scale ocean', *Non-linearity*, **5**, 1007–1053 (1992).
20. J.L. Lions, R. Temam and S. Wang, 'Models for the coupled atmosphere and ocean', in: *Computational Mechanics Advances*, vol. 1, North-Holland, Amsterdam, 1993, pp. 5–54.
21. F. Abergel and R. Temam, 'On some control problems in fluid mechanics', *Theor. Comput. Fluid Dyn.*, **1**, 303–325 (1990).
22. S.S. Ravindran, 'Numerical solutions of optimal control for thermally convective flows', *Int. J. Numer. Methods Fluids*, **25**, 205–223 (1997).

